JOURNAL OF MATERIALS SCIENCE **35** (2000) 2833–2839

Direct synthesis of potassium tantalate thin films by hydrothermal-electrochemical method

Z-B. WU, T. TSUKADA, M. YOSHIMURA*
Center for Materials Design, Materials and Structures Laboratory, Tokyo Institute of Technology, 4259 Nagatsuta, Midori-ku, Yokohama 226-8503, Japan
E-mail: Yoshimu1@rlem.titech.ac.jp

Single-phase potassium tantalate (KT) thin films with excellent film flatness and crystallinity have been synthesized on a tantalum substrate in 2.0 M KOH solution at 150°C by a hydrothermal-electrochemical method under a galvanostatic condition. A pyrochlore structure of the thin KT films was identified by XRD pattern analysis. The films show good adherence to the substrate and the film thickness could be as much as 2 μm. The electrical properties of the films were characterized through the determination of capacitance by electrochemical impedance spectroscopy at room temperature. Dielectric constants yielded from capacitance measurements have been calculated to have values higher than 300. The dependence of cell voltage on reaction time reflects the mechanism of film formation. The preparation conditions and morphology of the films were consistent with the proposed film formation mechanism.

1. Introduction

Potassium tantalate, known as an incipient ferroelectric material with a band gap energy of about 3.5 eV, has been the subject of extensive investigation because of its technological importance and fundamental interest [1–13]. A crystal of potassium tantalate shows a good n-type photoconductivity at low temperature. Excited by band-gap light at low temperature, a visible broad luminescent band can appear on an undoped $KTaO_3$ crystal surface [13]. Perovskite $KTaO_3$, similar to $SrCeO_3$, $BaCeO_3$ and $SrZrO_3$, is a high-temperature protonic conduction material when it is doped with a rare earth element. These materials have attracted considerable interest for possible applications to fuel cells, steam electrolyzes and humidity sensors [14–16]. Potassium tantalate can be used as a bulk substrate for high-T_c films [17]. Moreover, potassium tantalate films used in electric capacitors for DRAMs [18] have also been reported.

Potassium tantalate film and related compounds have previously been prepared by means of pulsed laser deposition [19], Liquid-Phase Epitaxy [20], and a sol-gel process [21, 22]. However, those film fabrication techniques are all capital and energy intensive because of the requirement of either a high vacuum or a temperature higher than 500°C.

In recent years, our group has been devoted to the development of hydrothermal and hydrothermal-electrochemical methods to fabricate in situ morphology-controlled crystalline ceramic films. These methods offer an alternative soft-chemical technique to fabricate thin as well as thick, shaped, sized and oriented ceramic films and coatings in aqueous solution for a variety of applications in one step without using excess energy for firing, sintering or melting. This simple ambient technique belongs to so-called the soft solution processing (SSP) [23, 24]. Typical examples are the formation of barium titanate and strontium titanate films on titanium substrates in alkaline solution by hydrothermal-electrochemical method [23, 24].

Many functional ceramic films have been prepared by a hydrothermal-electrochemical method recently [24], but to our knowledge, there is no published paper concerning the preparation of potassium tantalate films by a hydrothermal-electrochemical method. The purpose of this paper is to demonstrate the possibility of fabricating potassium tantalate by a hydrothermal-electrochemical method. The structure, morphology, and electrical properties of the films, as well as the mechanism of fabrication have been investigated.

2. Experimental procedure

Tantalum metal substrates of 99.9% purity and dimensions of 5 mm × 40 mm × 0.5 mm were used as working anodic electrodes. Prior to the hydrothermal-electrochemical treatment, the working electrode surface was polished by diamond and alumina suspensions successively to a mirror finish. The fresh polished electrode was electropolished for 30 seconds at an anodic current density of 1.5 mA/cm^2 in the electropolishing bath solution composed of 10 vol % H_2SO_4, 20 vol % HF, and 70 vol % ethylene glycol [25], the substrate was then ultrasonicated for 5 min in acetone and water

* Author to whom all correspondence should be addressed.

solutions. The hydrothermal-electrochemical treatment is described in detail elsewhere [26]. Briefly, a Teflon beaker containing the electrolyte was placed in the cell of an autoclave equipped with a three-electrode system. Ta and Pt plates served as the working electrode and counter electrode, respectively. A specially designed KCl-saturated Ag/AgCl electrode (Toshin Kogyo, Tokyo, Japan) was used as an external reference electrode. All potentials were referred to this reference electrode. Experiments were performed under galvanostatic conditions with the current density varied from 0.5 to 10 mA/cm^2 by a potentiostat (Potentiostat/Galvanostat 2000, Toho Technical Research). Changes in potential as a function of reaction time were recorded by a PC computer for selected experiments. Potassium hydroxide electrolyte solution was used in all experiments, freshly prepared from reagent grade potassium hydroxide and boiled distilled water. The temperature was controlled at 150°C, and the reaction cell was kept at the saturated vapor pressure at this temperature. After each experiment, the Ta substrate covered with the potassium tantalate film was washed with water, ultrasonically in ethanol, and air-dried prior to characterization.

X-ray diffraction was used to characterize the resultant phases of the products. A standard X-ray power diffractometer (Model MXP^{3VA}, MAC Science Co., Ltd., Tokyo, Japan) was used with Cu-K_α radiation at 40 KV and 40 mA at a scan rate of 1°/min from 10 to 80° 2θ. Both surface morphology and the thickness of the grown films were investigated both by scanning electron microscopy (SEM) (SEM, Model S-4000, Hitachi, Tokyo, Japan).

The electrochemical impedance spectroscopy for the samples of potassium tantalum oxide films on tantalum substrates were carried out by an EG&G PAR Model 273A potentiostat equipped with an EG&G model 5210 lock-in amplifier controlled by EG&G398 software through a PC computer. The experiments were conducted in 1.0 M KCl electrolyte solution (pH 7.0) at room temperature under argon atmosphere. A saturated calomel electrode (SCE) and a large-area platinum plate were used as the reference electrode and counter electrode, respectively. The working electrode with a thin film was immersed into the electrolyte except for the upper part, which was connected to the electrical circuit via a mechanical clamp. The geometric surface in contact with the solution was about 1.0 cm^2. The imposed ac signal was 5 mV rms, and the single sine model was fixed.

3. Results and discussion

3.1. Structure characterization

The smooth films obtained on an anodic tantalum substrate by hydrothermal-electrochemical galvanostatic treatment exhibited interference colors varying with the thickness. The X-ray diffraction pattern of one typical sample obtained by hydrothermal-electrochemical galvanostatic treatment in 2.0 M KOH solution for one hour at a current density of 1 mA/cm^2 is shown in Fig. 1, where the peaks of KT crystallites were indexed. All diffraction lines are well-defined without preferred orientations and show a single phase of crystalline cubic pyrochlore type potassium tantalum oxide film with the structural formula of $K_2Ta_2O_6$. The lattice parameter of this potassium tantalum oxide was determined to be $a = 10.5942$ A°, which is in good agreement with literature data [27]. The potassium carbonate phase was not observed. It is different from other dielectric films prepared by a hydrothermal or hydrothermal-electrochemical method, such as $BaTiO_3$ films. Sometimes, it is very difficult to avoid the contamination by barium carbonate [28–31]. Current study results obviously benefit from the solubility of potassium carbonate.

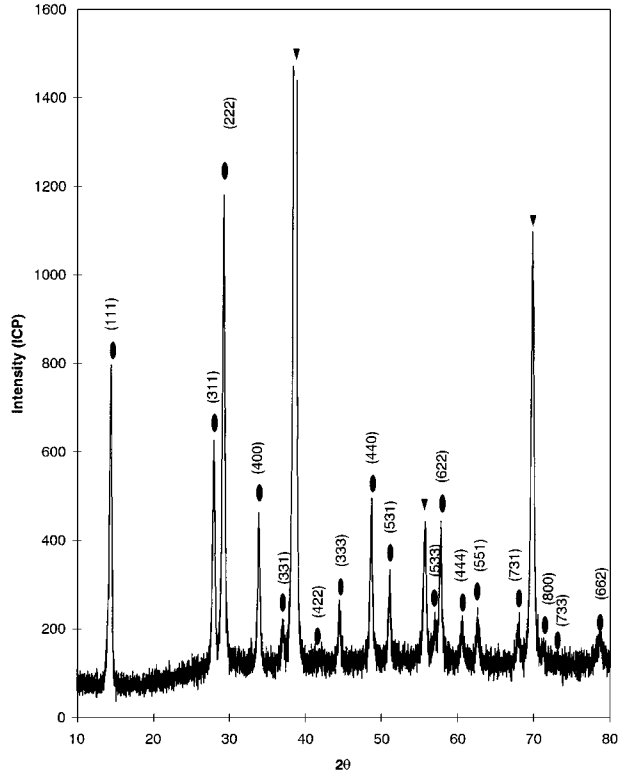

Figure 1 X-ray diffraction pattern of a potassium tantalum thin film on a Ta substrate. The peaks marked by and triangle are substrate peaks. KT film produced at 1 mA/cm^2 for 1 hour at 150°C by hydrothermal-electrochemical method.

Materials with a pyrochlore structure offer the potential properties for catalysis, ferroelectricity, ferromagnetism, luminescence and ionic conductivity [32–35]. The pyrochlore structure is cubic with the space group of Fd3m. Eight formula units of $A_2B_2X_6Y$ per unit cell is the ideal pyrochlore structural formula, where A and B are metal cations and X and Y are anions. The structure consists of a network of BX_6 octahedra sharing all their corners around hexagonal vacancies, and the lattice of an A_4Y tetrahedron positioned inside the vacancies [36]. The defect structures with the structural formula $A_2B_2X_6$ could be produced by removing the combination of A and Y ions. $K_2Ta_2O_6$ belongs to this type. Hirano *et al.* [21] reported the XRD profiles of potassium tantalum oxide powders prepared by the sol-gel process. The structure of potassium tantalate was changed by temperature from pyrochlore to perovskite. When fired at 650°C, the potassium tantalate exhibited the pyrochlore structure, and the formation of the perovskite $KTaO_3$ phase occurred at 850°C. The results

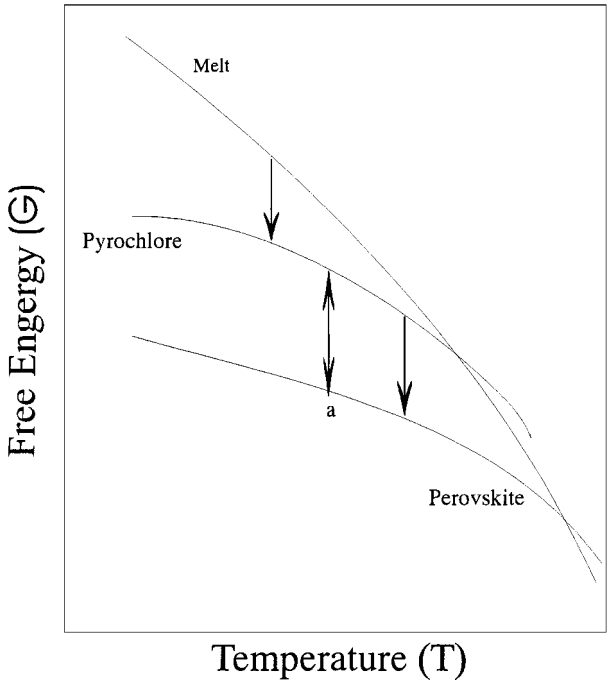

Figure 2 Schematically illustration the relationship between free energy and temperature for potassium tantalate system. Point a indicates the temperature (≈850°C) of reversible transformation between pyrochlore and perovskite phase.

indicated that the pyrochlore phase readily forms at lower temperature. However, Swartz's results showed that the pyrochlore potassium tantalum oxide structure can be formed in a sample crystallized from the glass composition $4KTaO_3 \cdot Al_2O_3$ after heating at 850°C for 30 minutes [28]. According to the lattice energy and apparent bond valence calculation [37], perovskite $KTaO_3$ is more stabler than pyrochlore $K_2Ta_2O_6$ in view of the lattice energy and apparent bond valence. Our results confirm that the pyrochlore structure is a sub-stable phase of potassium tantalate at low temperature. The relationship between free energy and temperature in the potassium tantalate system might be schematically expressed as that shown in Fig. 2. It is shown that the pyrochlore type structure, $K_2Ta_2O_6$ could predominately form at lower temperature. At a temperature of about 850°C (point a in Fig. 2), pyrochlore $K_2Ta_2O_6$ could reversibly transform to the perovskite structure, but this transformation becomes irreversible as soon as the temperature becomes higher than 850°C.

The scanning electron micrographs of the surface and cross section of the KT film hydrothermal-electrochemically produced at 1 mA/cm^2 for 2 hours are shown in Fig. 3. The film surface (Fig. 3a) is homogeneous and closely packed with well-defined octahedral submicrograins of KT. The more enlarged image (Fig. 3b) shows that the grain size is not uniform. The largest grains have a size of up to 0.4 μm. The average grain size is about 0.2 μm calculated by an intercept method. Fig. 3b also shows that the upper grains are bigger than the lower ones. The larger grains are located on the outer surface while the smaller ones are retained among the bigger ones. This type of microstructure may indicate that the grain growth mechanism is controlled by a nucleation and growth process, because the largest grains are those that nucleated first and thus have enough time to grow. The fine grains observed in the inner portion of the film also indicated that the film is grown from the outer surface to the inner. The cross sectional image of the film is shown in Fig. 3c. The thickness is evaluated about 2.0 μm.

3.2. Impedance spectroscopy

Generally, an equivalent electrical circuit, which is shown in the inset of Fig. 4a, is valid for illustration of the impedance behavior of the metal/oxide films/electrolyte interface. This circuit includes the elements of film resistance(R_f) and capacitance (C_f), Helmholtz capacitance (C_h) and the electrolyte resistance (R_s). When the R_f values are very high, the total impedance of the system can be written in the form [38, 39]:

$$Z = R_s - j\frac{1}{\omega}\left(\frac{1}{C_f} + \frac{1}{C_h}\right) = R_s - j\frac{1}{\omega C} \quad (1)$$

Therefore,

$$Z_{im} = \frac{1}{\omega C} \quad (2)$$

$$\log(Z_{im}) = -\log(f) - \log(2\pi C) \quad (3)$$

The linear dependence of $\log(Z_{im})$ with $\log(f)$ can be observed. When $C_h \gg C_f$, the contribution of C_h to the total capacitance (C) could be neglected. The calculation of C_f can hence be straightforwardly done from imaginary impedance data.

Impedance experiments for KT films were carried out at 0.0 V in 1.0 M KCl electrolyte solution (pH 7.0) under argon atmosphere at room temperature. Films were well-prepared and carefully selected to avoid any cracks containing in the film. Fig. 4a shows typical curves of the dependence of the impedance, $\log[Z]$, and phase angle, θ, on frequency $\log(f)$ for KT films of various thickness. At $f < 10$ K, a straight line was observed. The slope of the linearity depends on the film thickness. Simultaneously, at high frequency f, the phase angle θ was close to zero degree which corresponds to resistive behavior, whereas at $f < 100$ Hz, θ diminishes to values close to $-90°$, which correspond to capacitor behavior. Fig. 4b shows the good linearity relationship between the $\log(-Z_{im})$ and $\log(f)$ for different film thicknesses. The slopes of these plots were near to -1, which were in good agreement with the Equation 3. This indicated that the system actually behaved as an RC series circuit. From Fig. 4b, the capacitance values of the samples I, II, III were estimated to be 0.15, 0.29, and 0.46 μF/cm^2 corresponding to film thicknesses of 2.0, 1.2, and 0.6 μm. It is noted that the resistance of the films composed of dielectric materials is very high. For example, the resistivities for a 0.4 μm thick $BaTiO_3$ film could be as high as 10^{12} Ω·cm [40]. Therefore, the RC series circuit behavior of the KT films can be is considered as an effect of the high resistance of the films. On the other hand, it is noted that all values of obtained capacitance were lower than 1.0 μF/cm^2.

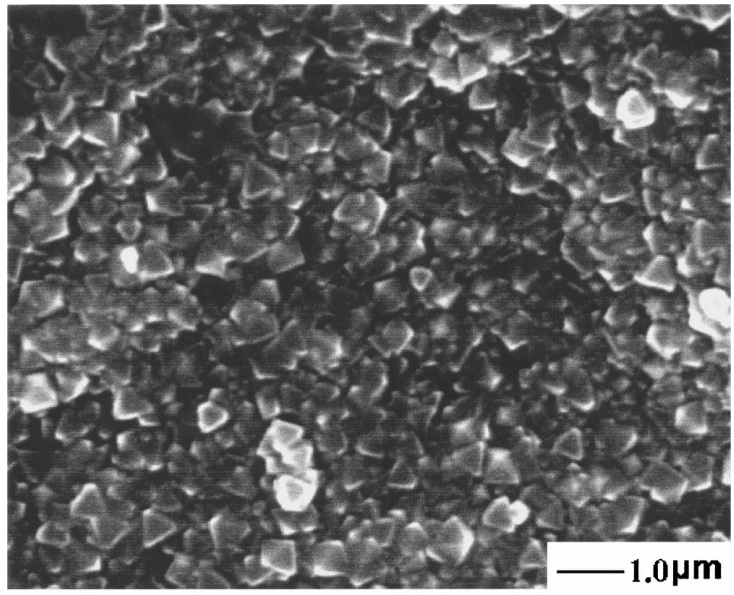

(a)

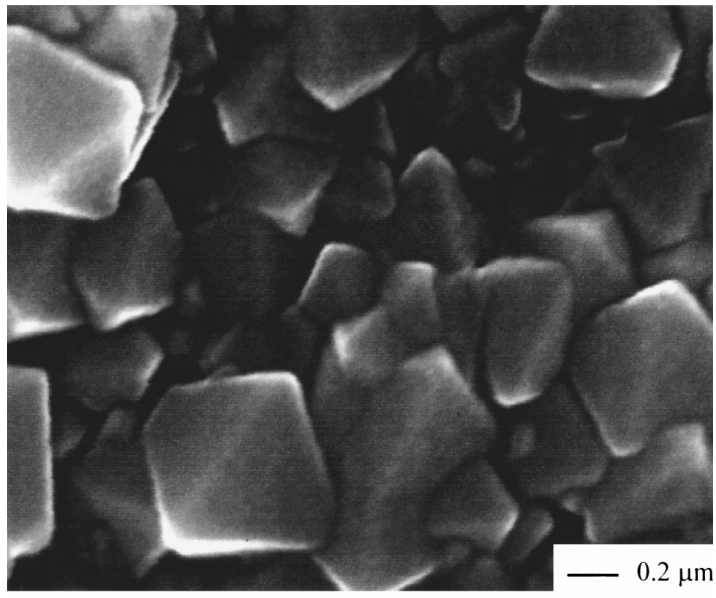

(b)

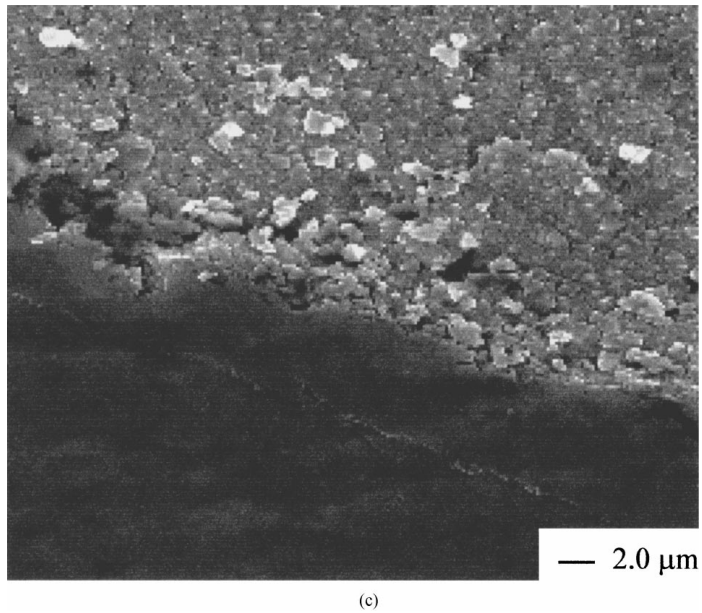

(c)

Figure 3 Scanning electron micrographs of the surface and cross section of KT film. KT film hydrothermal-electrochemically produced at 1 mA/cm^2 for 2 hour. a, b are correspondence with different magnification and c shows the cross section of the film.

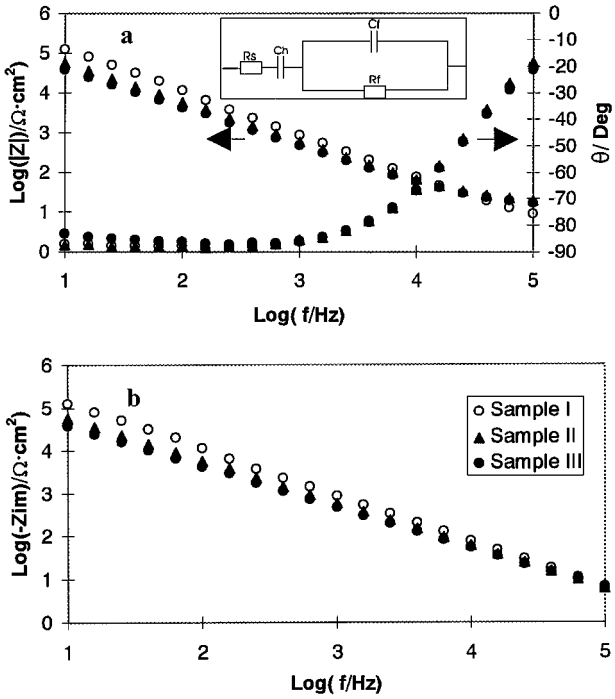

Figure 4 (a) Bode plots for KT films with various thickness. Insert is an equivalent electrical circuit proposed to describe the impedance behavior of the Ta metal/KT film/electrolyte interface. R_s is the uncompensated ohmic resistance of electrolyte and electrode, C_h is the Helmholtz capacitance. R_f and C_f are the film resistance and capacitance. (b) Frequency dependence of imaginary impedance Z_{im} for different film thickness. Sample I, II and III correspond the thickness of 0.6, 1.2 and 2.0 μm, respectively.

Because the values of the Helmholtz capacitance for the usual system are from 1.0×10^{-5} to 1.0×10^{-4} F/cm^2 [39], the lower system capacitance implies that the KT film capacitance is the main contribution of the whole system capacitance so that the influence of the Helmholtz capacitance can be neglected in this system. As a result, $C_f \approx C$, and the dielectric constant, ε, can be calculated directly from the capacitance obtained by the plot of Fig. 4b using the equation:

$$C = \frac{\varepsilon_0 \varepsilon}{d} \tag{4}$$

where $\varepsilon_0 = 8.85 \times 10^{-14}$ F/cm. Therefore, the dielectric constants for pyrochlore potassium tantalate films of samples I, II, III were calculated to be 312, 366, and 338, respectively. It was found that there is no apparent dependence of the dielectric constant on film thickness. The dielectric constants for the dielectric ceramic films, such as $BaTiO_3$ thin films, formed by a hydrothermal-electrochemical method varies from one research group to another, but usually, they are at values around 300 [29, 40–43]. The dielectric constant of the perovskite structure of $KTaO_3$ was determined to be 292 at 296°K [44]. The dielectric constant values obtained in the present study for the KT film are comparable to those measured for other dielectric films prepared by an electrochemical-hydrothermal method.

3.3. Discussion the film formation mechanism

Fig. 5 shows the potential change observed during the anodization of a Ta electrode in 2.0 M KOH solution

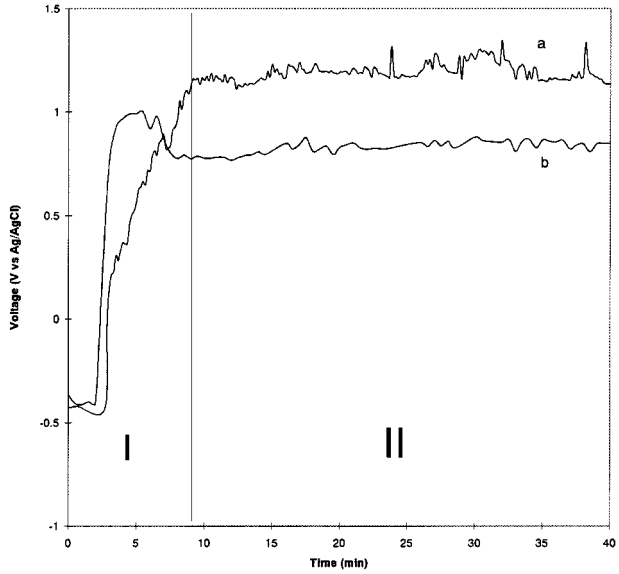

Figure 5 Plot of the cell potential against the time of reaction time for hydrothermal-electrochemical synthesis KT film under the constant current density of (a) 0.5, (b) 2.0 mA/cm^2 respectively.

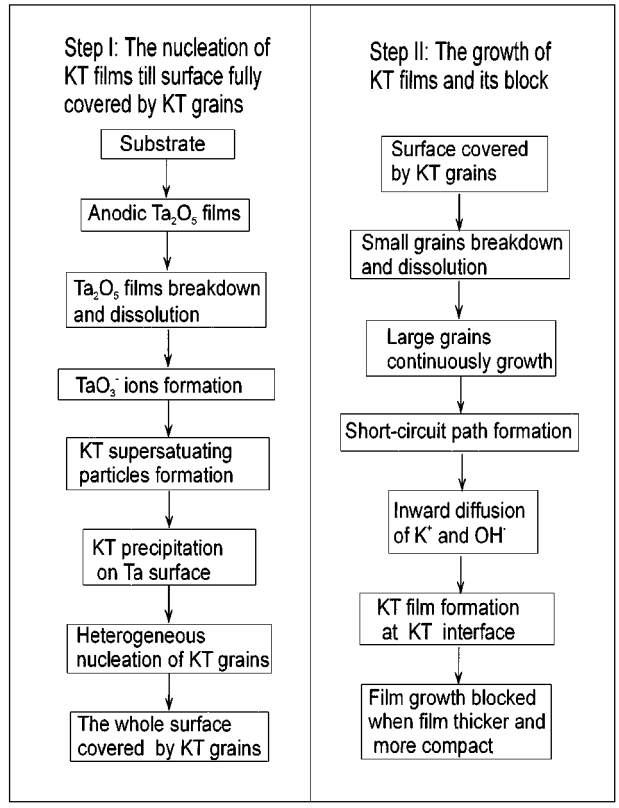

Figure 6 Schematically illustration of the mechanisms for hydrothermal-electrochemical synthesis of KT films on Ta substrate. See text for details.

at two current densities of 0.5 and 1.0 mA/cm^2. This dependence can be divided into two parts which are marked in Fig. 5, which are associated with the two steps of the KT film mechanism. The whole procedures are schematically displayed in Fig. 6. Step I in Fig. 6 is concerned with the processes of the initial formation of the KT precipitates and the heterogeneous nucleation of KT crystals on the substrate surface until all of the substrate surface is covered. As shown in Fig. 5, in step I, before current is input to the tantalum substrate,

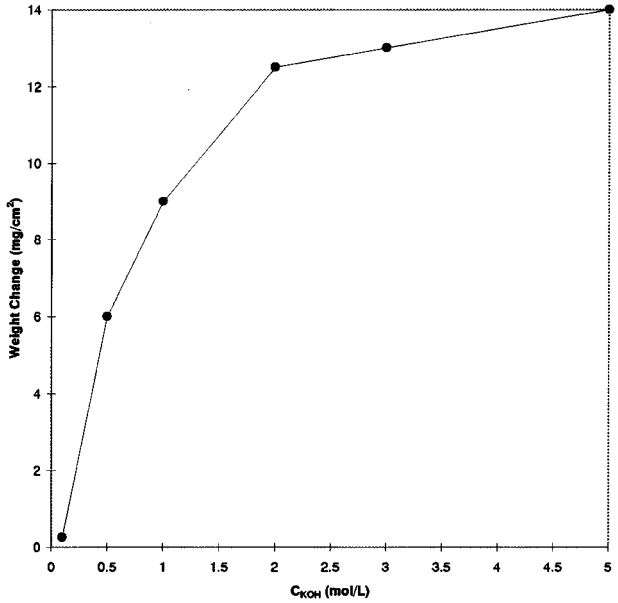

Figure 7 Dependence of the electrode weight change on the KOH concentration. The charge flowed into the electrode is 7.2 C/cm^2.

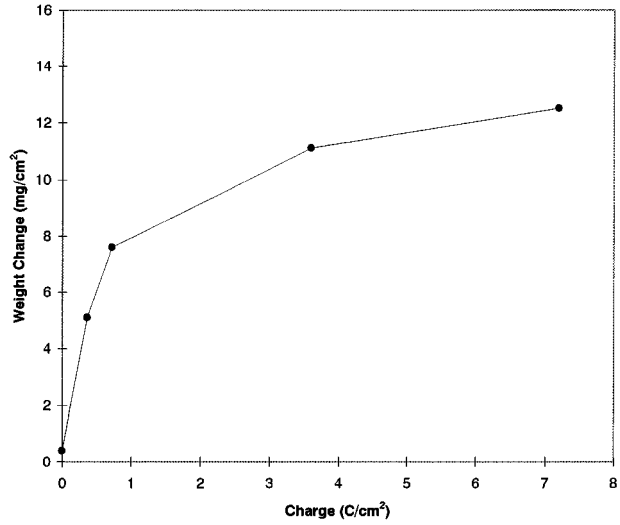

Figure 8 Dependence of the electrode weight change on the electric charge. 2.0 M KOH.

the amount of tantalum oxide on the Ta substrate is expected to be quite low except for the automatic formation under the hydrothermal condition. The insulating tantalum pentoxide films are grown fast once a constant current flows through the tantalum anode electrode, causing an increased voltage drop in the system. As the anodic potential increases to a certain value, the so-called breakdown potential, the tantalum oxide films would break down, which results in tantalum pentoxide dissolution in the concentrated alkaline solution to form TaO_3^- ion. According to Pourbaix's diagram [43], tantalum pentoxide actually is a protective oxide with high stability. It can resist caustic alkali solutions but dissolves in concentrated KOH solution to form TaO_3^- ion. It is believed that the higher concentrated alkaline media accelerate the dissolution of tantalum pentoxide and the formation of the KT film. In other words, this technique is highly dependent on the KOH concentration. This is consistent with the experimental results on the dependence of the electrode weight changes on the KOH concentration, shown in Fig. 7. Fig. 7 shows that KT films are hardly formed at a KOH concentration below 2.0 M, but there is no significant difference in the weight changes when the KOH concentration is higher than 2.0 M. Simultaneously, in step I, the dissolved TaO_3^- ions react with K^+ in the solution in the vicinity to form the double oxide $KTaO_3$ supersaturated particles which deposit on the Ta surface. The heterogeneous nucleation of KT crystals from the solution continues until the surface is fully covered with KT grains. As a result, the dissolution of tantalum oxide is somewhat blocked. It is believed that in this step the rate-determining reactions are the formation of tantalum pentoxide films and the growth of KT grains. The oxide dissolution and the precipitation of KT precipitates is suggested to be very fast because the dissolution is accelerated both by the electric field and the high hydroxyl concentration and there is much free space for depositing the supersaturated KT particles.

After the whole surface is covered by KT grains, the processes is assumed to proceed to the second step (Fig. 6). In Fig. 5, the voltage oscillation as a function of time is observed. It is believed that these oscillations are due to the breakdown of the films [31]. Because the tantalum pentoxide has already been blocked by the freshly formed KT grains, the breakdown could be attributed to the breakdown of the KT film and the dissolution of the KT grains. This favors the growth of the crystallites in the outer surface (Fig. 3b). Initially, when the KT film is very thin, this breakdown may cause exposure of the fresh tantalum oxide surface in order to form the new fine grains in the interior. Fig. 8 shows the dependence of the electrode weight change on the electrical charge. This figure exhibits the relationship of the KT film growth rate to the electrical charge or time under a constant current condition. It is shown that, at first, the film growth is fast with an almost linear relationship to charge, then slows down with time. When the substrate surface is completely covered by the KT grains, the successively formed supersaturated KT particles are thought to prefer to nucleate at the formed KT grain boundaries to provide a pathway or a so-called short-circuit path for the inward diffusion of K^+ and OH^- to the KT/Ta surface. This inward diffusion is much faster than that from the bulk crystals of KT. This diffusion supplies many K^+ and OH^- ions to the KT/Ta interface to produce a probably amorphous KT film (Fig. 3c) at this interface and cause the film to thicken. At this stage, the film still continues growing. However, the growth rate is gradually hindered by increasing the thickness of the KT film because the short-circuit paths become too narrow to transport K^+ and OH^- ions, specially when the film is highly packed.

4. Conclusions

In this paper, we have demonstrated the procedures of successfully fabricating potassium tantalate thin films by a hydrothermal-electrochemical method. This technique provides an inexpensive and environmentally friendly route to directly synthesize, dense, well

crystallized, single-phase films without post annealing. Benefiting from the solubility of potassium carbonate, the obtained films exhibit very pure film composition. Films with pyrochlore structure exhibit good adherence to the substrate and the film thickness can be up to 2 μm. The KT films shows higher dielectric constants with values higher than 300 which are independent of the film thickness. Based on the experimental results, it is concluded that the formation and growth of KT films by the hydrothermal-electrochemical method involve a dissolution-crystallization mechanism which includes several successive processes.

Acknowledgements

This work was supported by the Japanese Society for the Promotion of Science (JSPS) on the "Research for the Future" Program No. 96R06901. The authors would like to thank Mr. T. Watanabe and Mr. K. Sakai for experimental assistance and Dr. K-S. Han for valuable discussions.

References

1. M. KITAMURA and H. CHEN, *Ferroelectrics* **206/207** (1998) 55.
2. V. S. VIKHNIN, *ibid*. **199** (1997) 25.
3. D. J. SINGH, *ibid*. **194** (1997) 299.
4. H. VOGT, *ibid*. **202** (1997) 157.
5. *Idem*., *ibid*. **184** (1996) 31.
6. C. AUF DER HORST, S. MAGNIEN and S. KAPPHAN, *ibid*. **185** (1996) 265.
7. V. VIKHNIN, V. TREPAKOV, F. SMUTNY and L. JASTRABIK, *ibid*. **176** (1996) 7.
8. A. HAVRANEK and M. MARVAN, *ibid*. **176** (1996) 25.
9. A. V. POSTNIKOV, T. NEUMANN and G. BORSTEL, *ibid*. **164** (1995) 101.
10. B. SALCE, J. L. GRAVIL and L. A. BOATNER, *J. Phys.: Condens. Matter* **6** (1994) 4077.
11. Y. NISHIHATA, O. KAMISHIMA, H. MAEDA, T. ISHII, A. SAWADA and H. TERAUCHI, *Physica B* **208/209** (1995) 311.
12. Y. NISHIHATA, O. KAMISHIMA, K. OJIMA, A. SWADA, H. MAEDA and H. TERAUCHI, *J. Phys.: Condens. Matter* **6** (1994) 9317.
13. E. YAMAICHI, S. OHNO and K. OHI, *Jpn. J. Appl. Phys*. **27** (1988) 583.
14. S. Q. FU, W-K. LEE, A. S. NOWICK, L. A. BOATNER and M. M. ABRAHAM, *J. Solid State Chem.* **83** (1989) 221.
15. W-K. LEE, A. S. NOWICK and L. A. BOATNER, *Solid State Ionics* **18/19** (1986) 989.
16. H. ENGSTROM, J. B. BATES and L. A. BOATNER, *J. Chem. Phys*. **73** (1980) 1073.
17. R. FEENSTRA, L. A. BOANTNER, J. D. BUDAI, D. K. CHRISTEN, M. D. GALLOWAY and D. B. POKER, *Appl. Phys. Letter*. **54** (1989) 1063.
18. K. NAKAMURA and K. IMAI, *Jpn. Kokai Tokkyo Koho JP* 08, 195,328 [96,195,328].
19. H.-M. CHRISTEN, L. A. BOATNER, J. D. BUDAI, M. F. CHISHOLM, L. A. GEA, P. J. MARRERO and D. P. NORTON, *Appl. Phys. Ltter*. **68** (1996) 1488.
20. J. HULIGER, R. GUTMANN and P. WAGLI, *Thin Solid Films* **175** (1989) 201.
21. S. HIRANO, T. YOGO, K. KIKUTA, T. MORSHITA and Y. ITO, *J. Am. Ceram. Soc*. **75** (1992) 1701.
22. C. J. LU, A. X. KUANG, G. Y. HUANG and S. M. WANG, *J. Mater. Sci*. **31** (1996) 3081.
23. M. YOSHIMURA, *J. Mater. Res*. **13** (1998) 796.
24. M. YOSHIMURA and W. SUCHANEK, *Solid State Ionic* **98** (1997) 197.
25. H. V. K. UDUPA and V. K. VENIKATESAN, in "Encyclopedia of Electrochemistry of the Elements" Vol. II edited by Allen J. Bard (Marcel Dekker, INC, New York, 1974) p. 53.
26. K. KAJIYOSHI, TOMONO, Y. HAMAJI, T. KASANAMI and M. YOSHIMURA, *J. Am. Ceram. Soc*. **77** (1994) 2889.
27. Database of XRD instrument, Model MXP 3VA, MAC Science Co., LTD., Tokyo, Japan, PDF number is No. 351464.
28. R. R. BACSA, G. RUTSCH and J. P. DOUGHERTY, *J. Mater. Res*. **11** (1996) 194.
29. R. R. BACSA, P. RAVINDRANATHAN and J. P. DOUGHERTY, *ibid*. **7** (1992) 423.
30. S. VENIGALLA, P. BENDALE, J. R. AMBROSE, E. D. VERINK Jr. and J. H. ADAIR, *Mater. Res. Soc. Symp. Proc*. **243** (1992) 309.
31. P. BENDALE, S. VENGALA, J. R. AMBROSE, E. D. VERINK, Jr. and J. H. ADAIR, *J. Am. Ceram. Soc*. **76** (1993) 2619.
32. J. B. GOODENOUGH and R. N. CASTELLANO, *J. Solid State Chem*. **44** (1982) 108.
33. D. BERNARD, J. PANNETIER and J. LUCAS, *Ferroelectrics* **21** (1978) 429.
34. L. SODERHOLM, C. V. STAGER and J. E. GREEDAN, *J. Solid State Chem*. **43** (1982) 175.
35. N. CHEVALIER, F. GAUME-MAHN, J. JANIN and J. ORIOL, *C. R. Seances Acad. Sci., Ser. C* **255** (1962) 1096.
36. M. T. VANDENBORRE and E. HUSSON, *J. Solid State Chem*. **50** (1983) 362.
37. N. WAKIYA, Ph.D. Dissertation, Tokyo Institute of Technology, Japan, 1995.
38. J. MARSH and D. GORSE, *Electrochim. Atca* **43** (1997) 659.
39. C. DA FONSECA, S. BOUDIN and M. DA C. BELO, *J. Electroanal. Chem*. **379** (1994) 173.
40. K. KAJIYOSHI, Y. SAKABE and M. YOSHIMURA, *Jpn. J. Appl. Phys*. **36** (1997) 1209.
41. M. YOSHIMURA, S. E. YOO, M. HAYASHI and N. ISHIZAWA, *ibid*. **28** (1989) L2009.
42. S. VENIGALLA, P. BENDALE and J. H. ADAIR, *J. Electrochem. Soc*. **142** (1995) 2101.
43. T. KUROIWA, T. HONDA, H. WATARAI and K. SATO, *Jpn. J. Appl. Phys*. **31** (1992) 3025.
44. G. RUPPECHT and R. O. BELL, *Phys. Rev*. **3** (1964) A748.
45. M. POURBAIX, "Atlas of Electrochemical Equilibria in Aqueous Solutions" (National Association of Corrosion/Engineers, 2nd ed. Houston, TX, 1974) p. 251.

Received 15 January
and accepted 15 December 1999